Partial Model-Free Control of a 2-Input and 2-Output Helicopter System

Ying Xin*, Zhi-Chang Qin**, Wei-Guo Wu* and Jian-Qiao Sun ***
*Department of Mechanics, Tianjin University, Tianjin, China
**Department of Mechanics, Shandong University of Technology, Zibo, China
***School of Engineering, University of California, Merced, USA

Summary. This paper presents the partial model free control (MFC) design of a two-input two-output 2-DOF helicopter system. Within the framework of the model free control, a state-feedback strategy is designed to control the system. The system is assumed to be unknown and its dynamics are estimated from extensive measurements in real-time. Simulation results show that the model free control is an effective fault-tolerant approach and is able to achieve good tracking performance of the multi-input multi-output system. The control performances are also compared with the LQR control based on the nominal model of the system. The control effects of the numerical results for the partial model are quite promising.

Introduction

The traditional linear and nonlinear control techniques such as classical PID, backstepping and sliding mode control algorithms are model-based [1–3]. Model free approach is desirable and there have been quite some studies of model-free controls recently [4, 6–8]. The model-free control takes advantage of the fast algebraic parameter estimation combined with an ultra local model, avoiding using complex non-linear models in control design. The control scheme is valid for a small time window, and is updated in real time thanks to a fast estimator. The control law proposed consists of a PID controller augmented with compensating terms provided by the online estimation of the unknown system dynamics, leading to the so-called intelligent PID (iPID) control [9, 10]. The main advantage of the model-free control strategy is that it doesn't require neither prior knowledge of the system dynamics, nor complex parameters tuning [9].
Model-free control has been applied to many fields recently [11], such as dc/dc converters [10], active magic bearing [12], shape memory alloy [13], active braking control systems for two-wheeled vehicles [14], two-wheeled inverted pendulums [15], quadrotor UAV [16], two-dimensional planar manipulator [17] and the magnetic levitation system [18]. The model free control approach has also been applied to control the automotive engine and brake for stop-and-go scenarios [19]. Taking the position control of a shape memory alloy active spring, an experimental comparison of classical PID and model-free control have been done [20]. The stability margins of model-free control is studied by Flisee [21]. To deal with control of underactuated mechanical systems for stable limit cycles generation, a dual model-free controller is developed [22, 23]. The model free control method has also been applied to control unknown time delayed system [24]. The model-free control method proposed by Fliess is used to control systems with a single control variable and a single output variable [25]. To control systems with multi-input variables and multi-output variables (MIMO) with the model-free control method, the dynamics could be decomposed into multi-SISO systems. Each decoupled dynamics could be controlled by a designated nonlinear controller. Then the augmentation of the MFC can be utilized to control the MIMO system [26, 27]. The model-free controller with an observer is proposed for a class of uncertain continuous-time multi-input multi-output nonlinear dynamic systems [28]. A discrete-time formulation of the model-free control algorithm, named data-driven model-free control, is put forward in the framework of a MIMO system with azimuth and pitch position control loops [29–32]. In this paper, we take the model-free control method to control a MIMO nonlinear helicopter system. We assume that the system model is partially known so that it doesn't need to decompose the system into multi-SISO dynamics.
The structure of this paper is as following. A 2-DOF nonlinear helicopter system is presented in Section . Section reviews the model-free control method and introduces the model-control control design process for the MIMO system. The simulation and experimental results are presented in Section . At last, Section concludes the paper.

Modeling of the 2-DOF Helicopter System

A 2-input-2-output helicopter module made by Quanser company is shown in Figure 1. The nonlinear dynamic equations that describe the motions of the pitch and yaw motion with respect to the servo motor voltage can be written as

$$\begin{aligned}(J_{eq,p} + m_{heli}l_{cm}^2)\ddot{\theta} + m_{heli}l_{cm}^2\dot{\psi}^2\sin\theta\cos\theta + m_{heli}gl_{cm}\cos\theta \\ = K_{pp}V_{mp} + K_{py}V_{my} - B_p\dot{\theta}, \\ (J_{eq,y} + m_{heli}l_{cm}^2\cos^2\theta)\ddot{\psi} - 2m_{heli}l_{cm}^2\dot{\psi}\dot{\theta}\sin\theta\cos\theta \\ = K_{yp}V_{mp} + K_{yy}V_{my} - B_y\dot{\psi}.\end{aligned} \tag{1}$$

where the variables θ (pitch angle) and ψ (yaw angle) are generalized coordinates, V_{mp} and V_{my} are the input voltages acting on pitch and yaw servo motors respectively. Other specifications of the helicopter system are listed in Table 1.
Define a state vector $\mathbf{x}(t) = [\theta, \psi, \dot{\theta}, \dot{\psi}]^T$ and the dynamic equations can be packaged in matrix form

$$\dot{\mathbf{x}}(t) = \mathbf{A}(\mathbf{x})\mathbf{x} + \mathbf{G}(\mathbf{x}) + \mathbf{B}(\mathbf{x})\mathbf{u}(t), \tag{2}$$

where

$$\mathbf{A}(\mathbf{x}) = \begin{bmatrix} 0 & 0 & 1 & 0 \\ 0 & 0 & 0 & 1 \\ 0 & 0 & \frac{-B_p}{J_{eq,p}+m_{heli}l_{cm}^2} & \frac{-m_{heli}l_{cm}^2\dot{\psi}\sin\theta\cos\theta}{J_{eq,p}+m_{heli}l_{cm}^2} \\ 0 & 0 & \frac{2m_{heli}l_{cm}^2\dot{\psi}\sin\theta\cos\theta}{J_{eq,y}+m_{heli}l_{cm}^2\cos^2\theta} & \frac{-B_y}{J_{eq,y}+m_{heli}l_{cm}^2\cos^2\theta} \end{bmatrix}, \tag{3}$$

$$\mathbf{G}(\mathbf{x}) = \begin{bmatrix} 0 \\ 0 \\ \frac{-m_{heli}gl_{cm}\cos\theta}{J_{eq,p}+m_{heli}l_{cm}^2} \\ 0 \end{bmatrix}, \mathbf{u} = \begin{bmatrix} u_\theta \\ u_\psi \end{bmatrix} \tag{4}$$

$$\mathbf{B}(\mathbf{x}) = \begin{bmatrix} 0 & 0 \\ 0 & 0 \\ \frac{K_{pp}}{J_{eq,p}+m_{heli}l_{cm}^2} & \frac{K_{py}}{J_{eq,p}+m_{heli}l_{cm}^2} \\ \frac{K_{yp}}{J_{eq,y}+m_{heli}l_{cm}^2\cos^2\theta} & \frac{K_{yy}}{J_{eq,y}+m_{heli}l_{cm}^2\cos^2\theta} \end{bmatrix}. \tag{5}$$

The linear dynamic equations which have been linearized near the quiescent point ($\theta_0 = 0, \psi_0 = 0, \dot{\theta}_0 = 0, \dot{\psi}_0 = 0$) of the nonlinear Equation (1) can be written in state space,

$$\dot{\mathbf{x}} = \mathbf{A}_l\mathbf{x} + \mathbf{B}_l\mathbf{u}, \tag{6}$$

where

$$\mathbf{A}_l = \begin{bmatrix} 0 & 0 & 1 & 0 \\ 0 & 0 & 0 & 1 \\ 0 & 0 & \frac{-B_p}{J_{eq,p}+m_{heli}l_{cm}^2} & 0 \\ 0 & 0 & 0 & \frac{-B_y}{J_{eq,y}+m_{heli}l_{cm}^2} \end{bmatrix}, \tag{7}$$

$$\mathbf{B}_l = \begin{bmatrix} 0 & 0 \\ 0 & 0 \\ \frac{K_{pp}}{J_{eq,p}+m_{heli}l_{cm}^2} & \frac{K_{py}}{J_{eq,p}+m_{heli}l_{cm}^2} \\ \frac{K_{yp}}{J_{eq,y}+m_{heli}l_{cm}^2} & \frac{K_{yy}}{J_{eq,y}+m_{heli}l_{cm}^2} \end{bmatrix}. \tag{8}$$

Model-Free Control Design

Model free control has no physical model but a purely numerical model which involves very few parameters that are estimated online during operation of the plant. The feedback control law is built and tuned by the numerical model and is thus updated at each sample time. Model free control relies on the real-time estimation of derivatives of measured signals.

Review of SISO Model Free Control

The input-output relation of a single input single output (SISO) system could be represented by an first order local process model,

$$\dot{y}(t) = F(t) + \alpha u(t), \tag{9}$$

where $F(t)$ is a continuously updated value that represents the overall time-varying dynamics of the system, and it could be approximately estimated using the information from the control signal $u(t)$ and the controlled output $y(t)$ [25]. $\alpha > 0$ is a design parameter. The ideal value of α is set to the value of the exact model parameter b, assuming the exact model is $\dot{y}(t) = f(t) + bu(t)$.

The tracking error $e(t)$ is defined as

$$e(t) = y(t) - y_d(t),$$

where $y_d(t)$ is the desired tracking reference trajectory.

The key process of model-free control design is to estimate the differential $\dot{y}(t)$. As we all known, there are several math tools which could help us to finish this work, such the Taylor expansion and first order derivative plus lowpass filter technique.

Let T be the sample time of a digital system, and $p > 0$ be the bandwidth parameter of an anti-aliasing lowpass filter. The derivative of a measured signal can be computed by passing the measurement through the following transfer function,

$$H(s) = \frac{p}{s+p}s. \tag{10}$$

This filter generates the estimate of $\dot{y}(t)$, with the notation $[\dot{y}(t)]_{est}$, which leads to the modified expression of (9),

$$F_{est}\left(t\right)=\left[\dot{y}\left(t\right)\right]_{est}-\alpha u\left(t\right), \tag{11}$$

where $F_{est}\left(t\right)$ is the estimation of the unknown system dynamics $F\left(t\right)$. The derivative of the desired reference trajectory $\dot{y}_d(t)$ can also be generated with the lowpass filter described in (10).
In general, the model-free control input could be written as follows,

$$u=\frac{-F_{est}+\dot{y}_d+u_c}{\alpha}, \tag{12}$$

where u_c is the control input of the feedback controller need to be designed. By substituting (12) into (9),

$$\begin{aligned}\dot{y} &= F+\alpha(\frac{-F_{est}+\dot{y}_d+u_c}{\alpha}) \\ &= e_{est}+\dot{y}_d+u_c.\end{aligned} \tag{13}$$

where $e_{est}=F-F_{est}$ is the estimation error of the known system dynamics. The control structure is characterized by the following tracking error dynamics,

$$\dot{e}(t)=e_{est}+u_c. \tag{14}$$

If the system dynamics F can be estimated exactly, i.e. $e_{est}\approx 0$, the estimation error e_{est} can be seen as disturbance and the system output $y(t)$ will track $y_d(t)$ in finite time by designing the local controller u_c, such as iP, iPD, iPID methods, and so on.

Partial Model Free Control for MIMO Systems
For the 2-input 2-output helicopter system, we assume the matrix $\mathbf{B}(\mathbf{x})$ in Equation (6) is known prior and take the ultra-local model as follows,

$$\dot{\mathbf{y}}\left(t\right)=\mathbf{F}\left(t\right)+\alpha\mathbf{u}\left(t\right), \tag{15}$$

where $\mathbf{y}\left(t\right)=[\dot{\theta},\dot{\psi}]^T$ is the velocity part of the state variable $\mathbf{x}(t)$ defined previously, $\mathbf{F}\left(t\right)=[F_1(t),F_1(t)]^T$ is the matrix form of the system dynamics except the gravity part, $\mathbf{u}\left(t\right)\in\mathbf{R}^2$ is the control input, α is the last two rows of matrix $\mathbf{B}(\mathbf{x})$ and can be written as following,

$$\alpha=\left[\begin{array}{cc}\alpha_{11} & \alpha_{12}\\ \alpha_{21} & \alpha_{22}\end{array}\right]=\left[\begin{array}{cc}\frac{K_{pp}}{J_{eq,p}+m_{heli}l_{cm}^2} & \frac{K_{py}}{J_{eq,p}+m_{heli}l_{cm}^2}\\ \frac{K_{yp}}{J_{eq,y}+m_{heli}l_{cm}^2\cos^2\theta} & \frac{K_{yy}}{J_{eq,y}+m_{heli}l_{cm}^2\cos^2\theta}\end{array}\right]. \tag{16}$$

Then the state equation (6) of this helicopter system can be written as

$$\dot{\mathbf{x}}(t)=\left[\begin{array}{c}\mathbf{y}\left(t\right)\\ \mathbf{F}\left(t\right)\end{array}\right]+\left[\begin{array}{c}\mathbf{0}_{2\times2}\\ \alpha\end{array}\right]\mathbf{u}\left(t\right). \tag{17}$$

Based on the knowledge of model free control design for SISO system, we propose a partial model free control design method for the ultra-local system (15). We first estimate the derivative of $\mathbf{y}\left(t\right)$ by the lowpass filter (10). Then the system dynamics $\mathbf{F}\left(t\right)$ can be obtained from the derivative estimation and the control input,

$$\mathbf{F}_{est}\left(t\right)=\left[\dot{\mathbf{y}}\left(t\right)\right]_{est}-\alpha\mathbf{u}\left(t\right). \tag{18}$$

Then define the control input $\mathbf{u}(t)$ as the following form

$$\mathbf{u}\left(t\right)=\alpha^{-1}\left[-\mathbf{F}_{est}\left(t\right)+\dot{\mathbf{y}}_d\left(t\right)\right]+\mathbf{v}\left(t\right), \tag{19}$$

where $\dot{\mathbf{y}}_d\left(t\right)=[\ddot{\theta}_d,\ddot{\psi}_d]^T$ is the derivative estimation of $\mathbf{y}_d$, and $\mathbf{v}\left(t\right)\in\mathbf{R}^{2\times1}$ is a control vector need to be designed further. Substituting (19) into (15),

$$\begin{aligned}\dot{\mathbf{y}}(t) &= \mathbf{F}\left(t\right)-\mathbf{F}_{est}\left(t\right)+\dot{\mathbf{y}}_d\left(t\right)+\alpha\mathbf{v}\left(t\right) \\ &= \mathbf{e}_{est}+\dot{\mathbf{y}}_d\left(t\right)+\alpha\mathbf{v}\left(t\right).\end{aligned}$$

Define a tracking error state as $\mathbf{e}=\mathbf{x}-\mathbf{x}_d$. Substituting (19) into (17), the state equation can be transformed into error state as

$$\dot{\mathbf{e}}(t)=\left[\begin{array}{cc}\mathbf{0}_{2\times2} & \mathbf{I}_{2\times2}\\ \mathbf{0}_{2\times2} & \mathbf{0}_{2\times2}\end{array}\right]\mathbf{e}\left(t\right)+\left[\begin{array}{c}\mathbf{0}_{2\times1}\\ \mathbf{e}_{est}\end{array}\right]+\left[\begin{array}{c}\mathbf{0}_{2\times2}\\ \alpha\end{array}\right]\mathbf{v}(t). \tag{20}$$

When the estimation $\mathbf{F}_{est}\left(t\right)$ is enough close to the real system dynamics $\mathbf{F}\left(t\right)$, i.e. $\mathbf{e}_{est}\approx\mathbf{0}$, the complex nonlinear control design problem is translated to a linear control design problem. Lots of linear control design methods can be used to control the system (20). It is mentioned that the matrix α must be known prior and be invertible.

Simulation of the Control Strategy

The input voltages of the pitch and yaw motors with respect to the pitch and yaw control output u_θ and u_ψ are

$$V_{mp} = \begin{cases} V_{\theta,\min} & u_\theta \le V_{\theta,\min} \\ u_\theta & V_{\theta,\min} < u_\theta < V_{\theta,\max} \\ V_{\theta,\max} & u_\theta \ge V_{\theta,\max} \end{cases}, \tag{21}$$

$$V_{my} = \begin{cases} V_{\psi,\min} & u_\psi \le V_{\psi,\min} \\ u_\psi & V_{\psi,\min} < u_\psi < V_{\psi,\max} \\ V_{\psi,\max} & u_\psi \ge V_{\psi,\max} \end{cases}. \tag{22}$$

when using the UPM-2405 DC motor, the pitch control voltage u_θ is saturated by the maximum amplifier voltage $V_{\theta,\max} = 24V$ and the minimum voltage $V_{\theta,\min} = -24V$. Similarly, the yaw control voltage u_ψ when using the UPM-1503 DC motor is limited to a maximum voltage of $V_{\psi,\max} = 15V$ and a minimum voltage of $V_{\psi,\min} = -15V$.

LQR Control

To show the model free control performances of the MIMO helicopter system (2), we take the linear quadratic regulator (LQR) design as the comparison. A feed-forward and a proportional integral differential (FF+PID) control algorithms are designed to regular the pitch angle θ. A PID controller is designed to control the yaw angle ψ.

In FF+PID control, the pitch position is regulated using a nonlinear feed-forward loop that compensates for the gravitational torque $\tau_g = m_{hili} g l_{cm} \cos\theta$ in Equation (1). The feed-forward control is designed as

$$u_{ff} = k_{ff} \frac{m_{hili} g l_{cm} \cos\theta_d}{K_{pp}}, \tag{23}$$

where θ_d is the desired pitch angle and k_{ff} is the feed-forward control gain, here take $k_{ff} = 1.0$. This applies the bulk of the voltage needed to hover the helicopter at the commanded position.

An integrator is introduced to the feed back control to minimize the steady-state error. By introducing two extended state variables $x_5 = \int_0^t [\theta(\tau) - \theta_d(\tau)]\, d\tau$ and $x_6 = \int_0^t [\psi(\tau) - \psi_d(\tau)]\, d\tau$, the PID control $[u_{pid,\theta}, u_{pid,\psi}]^T = \mathbf{K}(\mathbf{x}_d - \mathbf{x})$ is designed, where

$$\mathbf{K} = \begin{bmatrix} k_{1p,\theta}, k_{1p,\psi}, k_{1d,\theta}, k_{1d,\psi}, k_{1i,\theta}, k_{1i,\psi} \\ k_{2p,\theta}, k_{2p,\psi}, k_{2d,\theta}, k_{2d,\psi}, k_{2i,\theta}, k_{2i,\psi} \end{bmatrix}, \tag{24}$$

Thus the control inputs can be expressed as

$$\begin{bmatrix} u_\theta \\ u_\psi \end{bmatrix} = \begin{bmatrix} u_{ff} \\ 0 \end{bmatrix} + \mathbf{K}(\mathbf{x}_d - \mathbf{x}). \tag{25}$$

Choosing appropriate weighting matrix $\mathbf{Q}$, $\mathbf{R}$ and considering the linearized state equation (6), the feedback control gain $\mathbf{K}$ can be solved as

$$\mathbf{K} = \begin{bmatrix} 18.9366, & 1.9798, & 7.4920, & 1.5280, & 7.0291, & 0.7696 \\ 2.2223, & 19.4458, & -0.4503, & 11.8933, & -0.7696, & 7.0291 \end{bmatrix}, \tag{26}$$

$$\mathbf{Q} = diag\left(\begin{bmatrix} 200, & 150, & 100, & 200, & 50, & 50 \end{bmatrix}\right), \tag{27}$$

$$\mathbf{R} = \begin{bmatrix} 1 & 0 \\ 0 & 1 \end{bmatrix}. \tag{28}$$

Partial MFC Method

With the model free design, the tracking control problem of the complex nonlinear MIMO dynamic system (1) have been transformed to control the linear equation (20). The next step we need to do is to design the control law $\mathbf{v}(t)$.

We also tale PID design method to design $\mathbf{v}(t)$. By introducing two extended state variables $e_5 = \int_0^t [\theta(\tau) - \theta_d(\tau)]\, d\tau$ and $e_6 = \int_0^t [\psi(\tau) - \psi_d(\tau)]\, d\tau$, the PID control law is

$$\mathbf{v}(t) = -\mathbf{P}\mathbf{e}(t), \tag{29}$$

where $\mathbf{P} \in \mathbf{R}^{2\times 6}$ is a feedback control gain matrix. However, from (5) and (16), we find the matrix α is not a constant matrix. In design process, we take its linearization, that is the last two rows of $\mathbf{B}_l$.

Choosing the same weighting matrix $\mathbf{Q}$, $\mathbf{R}$ in (27-28) and considering the coefficient matrix of error state equation (20), the feedback control gain $\mathbf{P}$ can also be solved as

$$\mathbf{P} = \begin{bmatrix} 18.7248 & 1.29871 & 0.7475 & 0.9424 & 7.0535 & 0.4984 \\ -1.3867 & 19.2759 & -0.9302 & 15.7588 & -0.4984 & 7.0535 \end{bmatrix}. \tag{30}$$

So the model free control law of the MIMO nonlinear helicopter system (15) is

$$\mathbf{u}(t) = \alpha^{-1}\left[-\mathbf{F}_{est}(t) + \dot{\mathbf{y}}_d(t)\right] - \mathbf{P}\mathbf{e}(t), \tag{31}$$

Simulation Results

In this subsection, we set two scenarios to simulate the 2-input 2-output nonlinear helicopter system (1) controlled with LQR and MFC methods respectively.

Scenario 1 Step Response Study

In this scenario, we set the tracking references $\theta_d(t)$ and $\psi_d(t)$ as

$$\theta_d(t) = 0, \psi_d(t) = 90^\circ. \tag{32}$$

Figure 2 shows the step reponses of angle θ and ψ respectively. From this figure, we can visually find that the pitch angle θ is well controlled with both LQR and MFC methods. However, it has a smaller overshoot of the yaw angle ψ controlled with MFC method. Figure 3 shows the control forces of u_θ and u_ψ respectively. In the subgraph of each subfigures, we find the control force generated with MFC method (red lines) has an oscillation at the beginning of the simulation. This is an usual phenomenon of MFC method because it need an estimation for system dynamics and it is a learning process.

Scenario 2 Complex Periodic Signal Tracking

We define two complex tracking reference trajectories for pitch angle and yaw angle,

$$\theta_d(t) = 0.3\sin(1.3t) + 0.1\cos(0.9t) + 0.2\sin(1.5t), \tag{33}$$

$$\psi_d(t) = 0.82 + 0.3\sin(1.6t) + 0.3\cos(0.6t) + 0.1\sin(0.8t). \tag{34}$$

With control gain $\mathbf{K}$, the feed-forward and the proportional integral differential (FF+PID) control voltage is added to the pitch servo motor to regular the pitch angle θ to track the reference trajectory (33). The PID control voltage is added to the yaw servo motor to control the yaw angle ψ to track the reference trajectory (34). The blue lines in Figure 4 and 5 are the tracking performances of pitch and yaw angle under LQR control respectively. The red lines in Figure 4 and 5 are the tracking performances of pitch and yaw angle with MFC method respectively. We find that the pitch and yaw angle θ and ψ controlled with MFC has fast response and smaller tracking errors compared to the LQR method. Figures 6 and 6 show the results of control force u_θ and u_ψ respectively. From these two figures we can still find the oscillation phenomenon at the beginning of simulation.

A Comparison Study

To investigate the improvement of the tracking performances, we set two evaluation functions. The two indexes will show the tracking control performances and the energy consumption of the controller. The smaller the $J_{\mathbf{x}}$ is, the better the tracking performances are. The smaller the $J_{\mathbf{u}}$ is, the lower energy consumption cost.

$$J_{\mathbf{x}} = \frac{1}{T}\int_0^T \left[\left(\theta(\tau) - \theta_d(\tau)\right)^2 + \left(\psi(\tau) - \psi_d(\tau)\right)^2\right] d\tau, \tag{35}$$

$$J_{\mathbf{u}} = \frac{1}{T}\int_0^T \left[|u_\theta(\tau)| + |u_\psi(\tau)|\right] d\tau. \tag{36}$$

In the simulation, we set simulation time $T = 50s$, the two indexes $J_{\mathbf{x}}$ and $J_{\mathbf{u}}$ of LQR and MFC are list in Table 2. Through the simulation results, we find that the MIMO nonlinear helicopter system controlled by model free control method would track the reference trajectories very well. Compared to LQR control from Table 2, the model free control improves the tracking performances quite a lot and the energy cost is nearly the same with the LQR control.

Conclusion

In this paper, a partial model-free output feedback controller was proposed to control a 2-DOF nonlinear helicopter system. The control strategy was implemented partly depends on the system model. A lowpass filter technique is applied to the differential estimation. Based on the proposed partial model-free control strategy, the linear quadratic regulator (LQR) technique is taken to optimize the control parameters. Two scenarios are set to check the control performances. From the study of the simulation, we find the control effects of the partial model-free control method are quite promising.

Acknowledgements

The material in this paper is based on work supported by grants (11172197, 11332008 and 11572215) from the National Natural Science Foundation of China.

References

[1] Åström, K. J., and Hägglund, T., 1995. *PID controllers: Theory, Design and Tuning*. Instrument Society of America Research Triangle Park, Nc.

[2] Madani, T., and Benallegue, A., 2006. "Backstepping control for a quadrotor helicopter". In Proceedings of International Conference on Intelligent Robots and Systems, pp. 3255–3260.

[3] Yang, J., Li, S., and Yu, X., 2013. "Sliding-mode control for systems with mismatched uncertainties via a disturbance observer". *IEEE Transactions on Industrial Electronics,* **60**(1), pp. 160–169.

[4] Bourdais, R., Fliess, M., Join, C., and Perruquetti, W., 2007. "Towards a model-free output tracking of switched nonlinear systems". *IFAC Proceedings Volumes,* **40**(12), pp. 504–509.

[5] Fliess, M., and Join, C., 2009. "Model-free control and intelligent PID controllers: towards a possible trivialization of nonlinear control?". *IFAC Proceedings Volumes,* **42**(10), pp. 1531–1550.

[6] Fliess, M., Join, C., and Sira-Ramirez, H., 2006. "Complex continuous nonlinear systems: their black box identification and their control". In Proceedings of the 14th IFAC Symposium on System Identification.

[7] Fliess, M., Join, C., and Sira-Ramirez, H., 2007. "Nonlinear estimation is easy". *International Journal of Modelling, Identification and Control,* **4**(1), pp. 12–27.

[8] Mboup, M., Join, C., and Fliess, M., 2009. "Numerical differentiation with annihilators in noisy environment". *Numerical Algorithms,* **50**(4), pp. 439–467.

[9] d'Andréa-Novel, B., Fliess, M., Join, C., Mounier, H., and Steux, B., 2010. "A mathematical explanation via "intelligent" PID controllers of the strange ubiquity of pids". In Proceedings of the Control & Automation, pp. 395–400.

[10] Michel, L., Join, C., Fliess, M., Sicard, P., and Chériti, A., 2010. "Model-free control of dc/dc converters". In Proceedings of the 12th Workshop on Control and Modeling for Power Electronics (COMPEL), Vol. 11, pp. 1–8.

[11] Fliess, M., Join, C., and Riachy, S., 2011. "Revisiting some practical issues in the implementation of model-free control". *IFAC Proceedings Volumes,* **44**(1), pp. 8589–8594.

[12] De Miras, J., Join, C., Fliess, M., Riachy, S., and Bonnet, S., 2013. "Active magnetic bearing: A new step for model-free control". In Proceedings of the 52nd IEEE Conference on Decision and Control, pp. 7449–7454.

[13] Gédouin, P.-A., Join, C., Delaleau, E., Bourgeot, J.-M., Arbab-Chirani, S., and Calloch, S., 2008. "Model-free control of shape memory alloys antagonistic actuators". *IFAC Proceedings Volumes,* **41**(2), pp. 4458–4463.

[14] Formentin, S., De Filippi, P., Tanelli, M., and Savaresi, S. M., 2010. "Model-free control for active braking systems in sport motorcycles". *IFAC Proceedings Volumes,* **43**(14), pp. 873–878.

[15] Yu, C. Y., and Wu, J. L., 2016. "Intelligent PID control for two-wheeled inverted pendulums". In Proceedings of the International Conference on System Science and Engineering (ICSSE), pp. 1–4.

[16] Younes, Y. A., Drak, A., Noura, H., Rabhi, A., and Hajjaji, A. E., 2014. "Model-free control of a quadrotor vehicle". In Proceedings of the International Conference on Unmanned Aircraft Systems (ICUAS), pp. 1126–1131.

[17] Madoński, R., and Herman, P., 2013. "Model-free control of a two-dimensional system based on uncertainty reconstruction and attenuation". In Proceedings of the 2013 Conference on Control and Fault-Tolerant Systems (SysTol), pp. 542–547.

[18] Moraes, M. S., and da Silva, P. S. P., 2015. "Model-free control of magnetic levitation systems through algebraic derivative estimation". In Proceedings of the 23rd ABCM International Congress of Mechanical Engineering.

[19] Choi, S., d'Andréa-Novel, B., Fliess, M., Mounier, H., and Villagra, J., 2009. "Model-free control of automotive engine and brake for stop-and-go scenarios". In Proceedings of the European Control Conference (ECC), pp. 3622–3627.

[20] Gédouin, P.-A., Delaleau, E., Bourgeot, J.-M., Join, C., Arbab-Chirani, S., and Calloch, S., 2011. "Experimental comparison of classical pid and model-free control: position control of a shape memory alloy active spring". *Control Engineering Practice,* **19**(5), pp. 433–441.

[21] Fliess, M., and Join, C., 2014. "Stability margins and model-free control: A first look". In Proceedings of the 2014 European Control Conference (ECC), pp. 454–459.

[22] Andary, S., and Chemori, A., 2011. "A dual model-free control of non-minimum phase systems for generation of stable limit cycles". In Proceedings of the Conference on Decision and Control and European Control Conference, pp. 1387 – 1392.

[23] Andary, S., Chemori, A., Benoit, M., and Sallantin, J., 2012. "A dual model-free control of underactuated mechanical systems, application to the inertia wheel inverted pendulum". In Proceedings of American Control Conference, Vol. 18, pp. 1029–1034.

[24] Doublet, M., Join, C., and Hamelin, F., 2016. "Model-free control for unknown delayed systems". In Proceedings of the 3rd Conference on Control and Fault-Tolerant Systems (SysTol), pp. 630–635.

[25] Fliess, M., and Join, C., 2013. "Model-free control". *International Journal of Control,* **86**(12), pp. 2228–2252.

[26] Younes, Y. A., Drak, A., Noura, H., Rabhi, A., and Hajjaji, A. E., 2016. "Robust model-free control applied to a quadrotor UAV". *Journal of Intelligent & Robotic Systems*, pp. 1–16.

[27] Precup, R.-E., Radac, M.-B., Roman, R.-C., and Petriu, E. M., 2017. "Model-free sliding mode control of nonlinear systems: Algorithms and experiments". *Information Sciences,* **381**, pp. 176–192.

[28] Boubakir, A., Labiod, S., Boudjema, F., and Plestan, F., 2014. "Model-free controller with an observer applied in real-time to a 3-DOF helicopter". *Turkish Journal of Electrical Engineering & Computer Sciences,* **22**(6), pp. 1564–1581.

[29] Radac, M.-B., Roman, R.-C., Precup, R.-E., and Petriu, E. M., 2014. "Data-driven model-free control of twin rotor aerodynamic systems: Algorithms and experiments". In Proceedings of the IEEE International Symposium on Intelligent Control (ISIC), pp. 1889–1894.

[30] Roman, R.-C., Radac, M.-B., Precup, R.-E., and Petriu, E. M., 2015. "Data-driven optimal model-free control of twin rotor aerodynamic systems". In Proceedings of the IEEE International Conference on Industrial Technology (ICIT), pp. 161–166.

[31] Roman, R. C., Radac, M. B., Precup, R. E., and Stinean, A. I., 2015. "Two data-driven control algorithms for a MIMO aerodynamic system with experimental validation". In Proceedings of the International Conference on System Theory, Control and Computing, pp. 736–741.

[32] Roman, R.-C., Radac, M.-B., and Precup, R.-E., 2016. "Multi-input–multi-output system experimental validation of model-free control and virtual reference feedback tuning techniques". *IET Control Theory & Applications,* **10**(12), pp. 1395–1403.

Table 1: The helicopter system specifications

Symbol	Description	Value	Unit
m_{heli}	total moving mass of the helicopter	1.3872	kg
l_{cm}	center of mass along helicopter body from pitch axis	0.1860	m
$J_{eq,p}$	total moment of inertia about pitch axis	0.0384	$kg.m^2$
$J_{eq,y}$	total moment of inertia about yaw axis	0.0432	$kg.m^2$
B_p	equivalent viscous damping about pitch axis	0.8000	N/V
B_y	equivalent viscous damping about yaw axis	0.3180	N/V
K_{pp}	thrust torque constant of pitch axis from pitch propeller	0.2040	$N.m/V$
K_{py}	thrust torque constant of pitch axis from yaw propeller	0.0068	$N.m/V$
K_{yy}	thrust torque constant of yaw axis from yaw propeller	0.0720	$N.m/V$
K_{yp}	thrust torque constant of yaw axis from pitch propeller	0.0219	$N.m/V$

Table 2: The evaluation function values

Index	Step-LQR	Step-MFC	Period-LQR	Period-MFC
J_x	91.2868	82.0765	97.9797	53.4541
$J_{\mathbf{u}}$	25.0748	25.0701	24.4156	24.2612

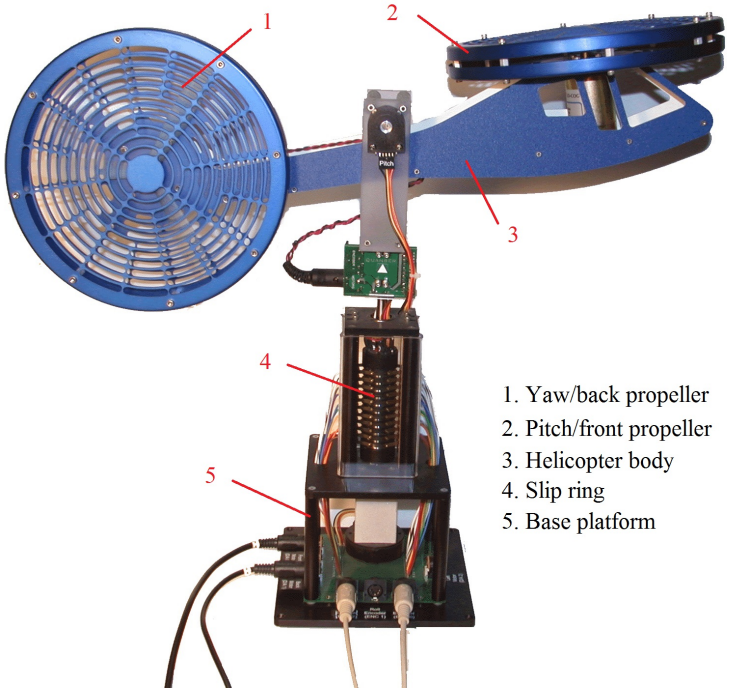

Figure 1: The module of 2-DOF helicopter system.

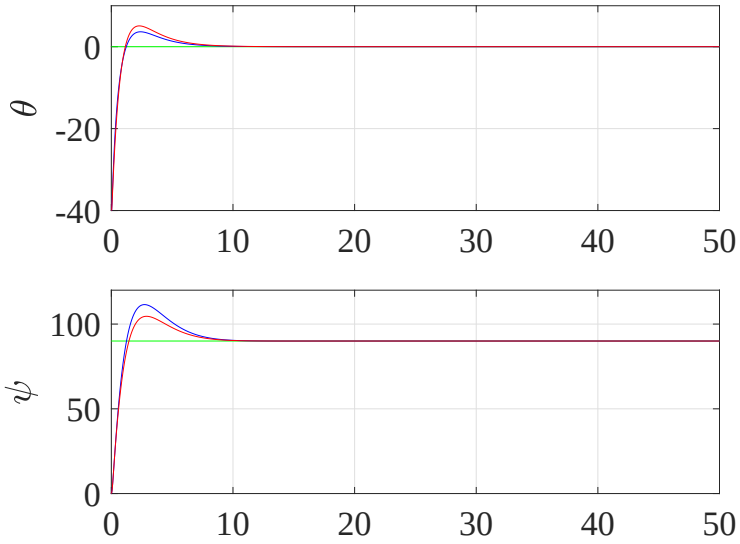

Figure 2: The simulation results of step response for angle $\theta(t)$ and $\psi(t)$ when tracking $\theta_d(t) = 0°$ and $\psi(t) = 90°$ respectively.

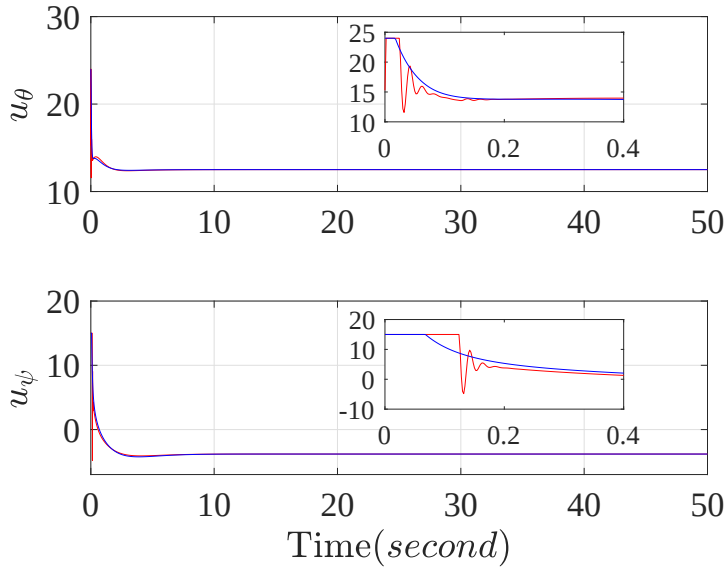

Figure 3: The control results of step response simulation. The blue lines are the LQR control forces and the red ones are model-free control forces. The oscillations of the red lines at the beginning of the simulation in the subgraph are introduced by the estimation of the system dynamics.

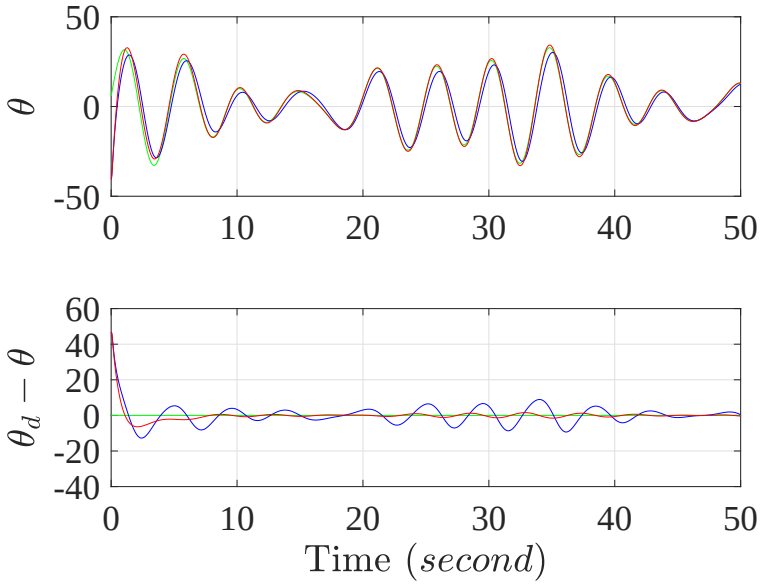

Figure 4: The simulation results of pitch angle and tracking error when tracking the reference signal $\theta_d(t)$. The gree line is the reference trajectory, the blue line is result controlled with LQR method and the red line represents the tracking performance controlled with MFC method.

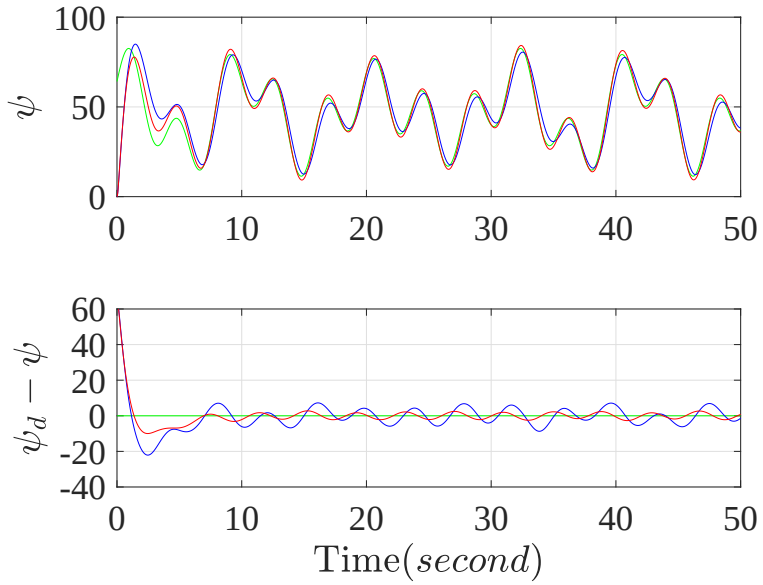

Figure 5: The simulation results of yaw angle and tracking error when tracking the reference signal $\psi_d(t)$. The gree line is the reference trajectory, the blue line is result controlled with LQR method and the red line represents the tracking performance controlled with MFC method.

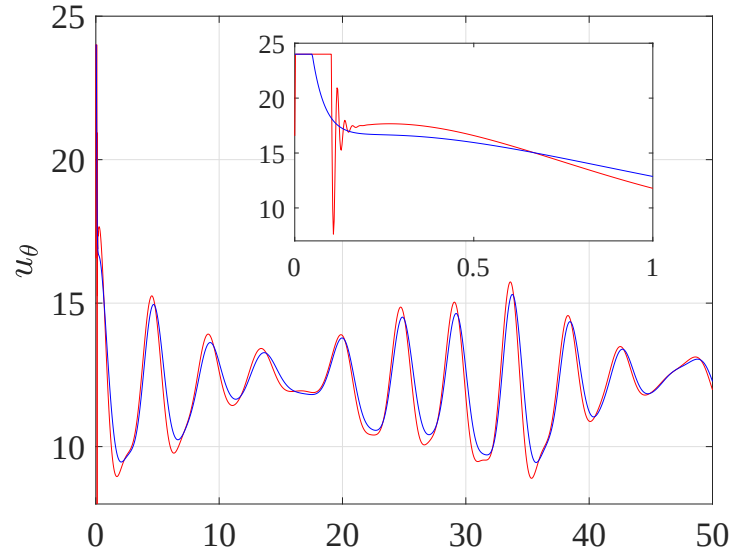

Figure 6: The simulation results of the control force u_θ. The blue line represents the control force generated by LQR method and the red line represents the control force generated by MFC method.

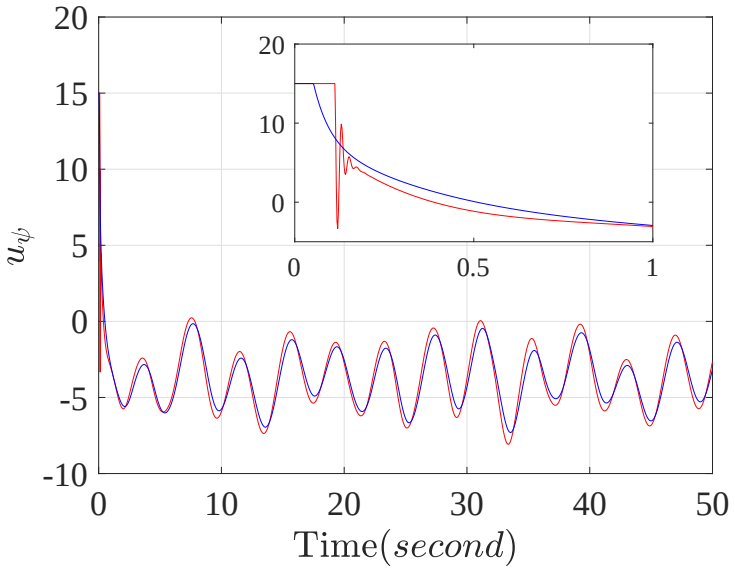

Figure 7: The simulation results of the control force u_ψ. The blue line is the control force of LQR control and the red line is the control force of model-free control.